

Remediation of the unsaturated zone of NAPL-polluted low permeability soils with steam injection: an experimental study

Dimitra N. Tzovolou · Christos A. Aggelopoulos ·
Maria A. Theodoropoulou · Christos D. Tsakiroglou

Received: 8 March 2010 / Accepted: 20 June 2010 / Published online: 9 July 2010
© Springer-Verlag 2010

Abstract

Purpose Although steam injection has been studied extensively as a potential technology for the remediation of soils polluted by hydrocarbons, there is still an ambiguity concerning the applicability of the method to unsaturated and low permeability soils. The goal of the present work is to identify the dominant mechanisms of pollutant removal and evaluate the effectiveness of steam injection for a mixture of semi-volatile and non-volatile hydrocarbons, and the unsaturated zone of low permeability soils. Such information is helpful for the interpretation of the results from relevant field-scale experiments.

Materials and methods An unsaturated and low permeability soil is polluted with a synthetic light non-aqueous phase liquid (LNAPL) which is a mixture of non-volatile and semi-volatile hydrocarbons: *n*-dodecane (*n*-C12), *n*-decane (*n*-C10), 1,2,4-trimethylbenzene, methylcyclohexane. The soil is packed in a tank (0.5 m×0.55 m×0.12 m) of poly-methyl-methacrylate, and two lenses of coarse-grained sand act as

high-permeability hydraulic fractures, with the steam being injected through the lower one and effluent (water/non-aqueous phase liquid (NAPL)/gas) being extracted from the upper one. After the completion of the test, a great number of soil samples are analyzed with gas chromatography–flame ionization detection to map the spatial distribution of the concentration of NAPL-compounds and evaluate the NAPL-removal efficiency.

Results and discussion The condensation of water in the pores of unsaturated soil may block the upward convective steam flow and alters locally the pore structure of the soil by creating high-permeability pathways. Thanks to these pathways, the upward flow of steam at high rates sweeps the vapors of NAPL (steam stripping) formed at temperatures lower than 100°C (steam distillation). The NAPL removal efficiency is satisfactory but non-uniform throughout the soil and is maximized in areas dominated by preferential flow paths and for the most volatile compounds. **Conclusions** In the unsaturated zone of a low-permeability soil, the removal of LNAPL with steam injection is enhanced in areas dominated by high-permeability preferential flow paths. The vaporization of semi-volatile and non-volatile compounds at temperatures lower than 100°C (steam distillation) coupled with steam stripping are the dominant mechanisms of LNAPL remediation.

Responsible editor: Jianming Xu

D. N. Tzovolou · C. A. Aggelopoulos · M. A. Theodoropoulou ·
C. D. Tsakiroglou (✉)
Foundation for Research and Technology Hellas-Institute of
Chemical Engineering and High Temperature Chemical Processes,
Stadiou str., Platani,
26504 Patras, Greece
e-mail: ctsakir@iceht.forth.gr

D. N. Tzovolou
e-mail: dtzovol@iceht.forth.gr

C. A. Aggelopoulos
e-mail: caggelop@iceht.forth.gr

M. A. Theodoropoulou
e-mail: mtheod@iceht.forth.gr

D. N. Tzovolou
Department of Chemistry, University of Patras,
26504 Patras, Greece

Keywords Hydraulic fracture · Non-aqueous phase liquid ·
Soil remediation · Steam distillation · Steam injection ·
Thermal treatment

1 Introduction

Steam injection was first developed by the petroleum industry for the enhanced recovery of oils from reservoir rocks (Farouq and Meldau 1979; Stewart and Udell 1988). During the last decades, steam injection has been tested as a

method to remediate non-aqueous phase liquids (NAPL)-contaminated sites (Hunt et al. 1988; Dablow et al. 2000; Heron et al. 2005). The main NAPL recovery mechanisms are (Davis 1998; Class et al. 2002): (1) the physical displacement by condensed water and steam itself (Hadim et al. 1993; Gudbjerg et al. 2004a); (2) the decrease of the interfacial tension and NAPL viscosity at elevated temperatures (She and Sleep 1998); (3) the steam distillation (Acierno et al. 2004); (4) the steam stripping (Braass et al. 2003); (5) the vaporization (Kuhlman 2002); (6) boiling-induced heat conduction from the steam zone (Gudbjerg et al. 2004b); and (7) the contaminant desorption from the solid phase (Tse et al. 2001).

Experimental and theoretical studies revealed that steam injection may be an efficient method for the remediation of soils from mixtures of volatile and semivolatile contaminants that have low solubility to water (Schmidt et al. 2002). However, the majority of field- and laboratory-scale studies of soil remediation by steam injection have been focused on the saturated zone of relatively high-permeability porous media (Tse et al. 2001; Gudbjerg et al. 2004a), and little attention has been paid on the remediation of the unsaturated zone (Schmidt et al. 2002). Theoretical (Falta et al. 1992) and one-dimensional experimental (Hadim et al. 1993) studies have revealed that hydrocarbons having boiling points up to 175°C (e.g., jet fuel) may be removed completely behind the steam condensation front. However, all these studies were focused on high-permeability and fully saturated soils where the physical displacement of pollutant by steam and condensed water was the dominant recovery mechanism.

In the unsaturated zone of low permeable soils, the NAPL transport is governed by preferential flow paths of the microporous matrix (Aggelopoulos and Tsakiroglou 2009) and fracture networks (Slough et al. 1999) both comprising a small percentage of the total porosity. After a long period of contamination, the target NAPL pollutants may be accumulated in the low permeable porous matrix which has limited accessibility to the high-permeability pathways (Totsche et al. 2003; Harrar et al. 2007). In this manner, the conventional vertical wells installed on low permeable media are expected to be inefficient as long as they do not intersect with the natural fractures and preferential flow paths. The NAPL-mass transfer coefficients (diffusion, dissolution, vaporization, etc.) for complicated microporous networks are so small (Hønning et al. 2007; Christiansen et al. 2008) that a long duration of soil treatment and a high density of wells are required to achieve an efficient remediation (Mercer and Cohen 1990). For this purpose, various stimulation technologies have been suggested with the hydraulic fracturing being the most promising one (Murdoch 1995; Hossain et al. 2000).

In spite of the field- and lab-scale studies of soil remediation with steam injection, no systematic effort has

ever been done to evaluate the efficiency of steam injection for the removal of NAPL from the unsaturated zone of low-permeability soils. In the present work, the steam is injected, and effluent is extracted through two horizontal hydraulic fractures placed within an unsaturated soil polluted by a 4-component synthetic LNAPL. The setup of experiment simulates the conditions of a pilot-scale test designed to evaluate the applicability of the method to heterogeneous soils contaminated by jetfuel. Our main goal is to identify the dominant mechanism of LNAPL-removal and evaluate the efficiency of steam injection for a mixture of semi-volatile and non-volatile hydrocarbons, and the unsaturated zone of low-permeability soils. This is of key importance for the interpretation of analogous pilot-scale experiments (Dablow et al. 2000) where the great variety of mass- and heat-transfer operations is not limited within the cell boundaries, and unavoidably, uncertainties are embedded into the estimated LNAPL-removal efficiency.

2 Materials and methods

2.1 Materials and experimental setup

Soil from the region of Western Greece (Kato Achaia) with the properties shown in Table 1 was air-dried and disposed of large debris. A synthetic NAPL was prepared by mixing *n*-decane, *n*-dodecane, methylcyclohexane, and 1,2,4-trimethylbenzene (Table 2). The dry soil was humidified by adding tap water in it up to a moisture close to 11% *w/w* (volumetric water saturation=14.2%). Afterwards, the wet soil was contaminated by mixing it with the synthetic NAPL at an average concentration 50 g/kg-soil (volumetric NAPL saturation=8.3%). Then the soil was packed inside a rectangular tank of poly-methyl-methacrylate (PMMA) with height=0.55 m, length=0.5 m and width =0.12 m (Fig. 1). First, the bottom of the tank was packed with a layer of water-saturated soil of 5-cm thickness. Afterwards, the NAPL-contaminated soil was packed layer by layer in the tank up to a thickness of 40 cm. Two “hydraulic” fractures of average aperture ~2 cm were created artificially at depths 10 and 40 cm from the bottom of the tank by packing coarse sand ($\langle d_g \rangle \sim 0.5$ cm). The permeability of the coarse sand (hydraulic fracture) was measured on a sandpack bed and found $\sim 1,200 \times 10^{-12}$ m², namely more than three orders of magnitude higher than the soil permeability (see Table 1). The contaminated soil was covered by a dry layer of soil, and the tank was sealed by tightening two screws on an aluminum plate placed on the PMMA cover plate (see Fig. 1). Care was taken to minimize the volatilization of VOCs (methylcyclohexane) during the packing and ensure uniform NAPL concentration throughout the soil (see Fig. 1).

Table 1 Soil properties

pH (1:1)*	Conductivity (S m ⁻¹)	Total organic carbon (TOC) (% w/w)	Total porosity (%)	Hg porosimetry porosity with $D_p < 2.15 \mu\text{m}^{**}$ (%)	Pore diameter distribution ($D_p < 2.15 \mu\text{m}$)	Permeability (m ²)	Bulk density (kg/m ³)	Grain size distribution (% w/w)
6.5	0.11	1.4	42.0	32.5	$<D_p > = 23 \mu\text{m}$ $<\sigma_p > = 53 \mu\text{m}$	385×10^{-15}	1580	$D_g > 125 \mu\text{m}$: 69% $50 \mu\text{m} < D_g < 125 \mu\text{m}$: 14% $2 \mu\text{m} < D_g < 50 \mu\text{m}$: 4% $D_g < 2 \mu\text{m}$: 13%

*Ratio of soil weight to tri-distilled water weight

**The maximum pore diameter detected with mercury intrusion porosimetry

Superheated dry steam of temperature ~140–150°C was produced in a batch steam generator with maximum water volume capacity 5 L, power 2 kW, and maximum pressure 8 bar. The steam was injected under an average rate of 0.4 kg/h, through a stainless steel tube inserted in the middle of the lower hydraulic fracture. Effluents were allowed to escape through a tube inserted in the middle of the upper hydraulic fracture. The effluents circulated through a condenser, and the liquid condensate was collected in a storage tank. The injection pressure along with the temperature at two horizontal positions were measured (see Fig. 1), whereas the experiment was video-recorded to visualize the steam flow paths along with potential changes caused in the soil structure. The steam injection experiment was conducted twice, whereas the experimental conditions were kept identical to ensure the repeatability of the results.

2.2 Chemical analyses

After the completion of the test, the soil started to be removed layer by layer, and 54 soil samples were collected from seven horizontal cross-sections and along five vertical directions. Twenty-seven pairs of samples were collected at distances 3 cm from the front (front side) and back (back side) PMMA plates of the tank. The concentration of the NAPL compounds in soil samples were measured with gas chromatography combined with flame ionization detector (GC-FID). Soon after sampling, the soil samples were precisely weighted (1.9 ± 0.4 g) and placed immediately into 7-ml amber glass vials capped with Teflon-faced silicon septa. In each vial, 4 ml of dichloromethane was added, and the vials were shaken for a couple of hours on an overhead shaker at a speed of 10 rpm. The organic solution was decanted to a clean vial, desiccated with the addition of Na₂SO₄, and filtered on 0.45- μm PTFE filters with one-way glass syringes. A GC-FID (GC 2014 Shimadzu), equipped with a fused silica capillary column was used to measure the concentrations of the four compounds of synthetic NAPL.

2.3 Calculation of the boiling points of NAPL compounds

The solubility of NAPL compounds in water is so low (see Table 2) that, for practical applications, the mixture of NAPL and water may be regarded as a system of immiscible fluids. Under such conditions, the vapor pressure of each component (NAPL and water) is not influenced by the presence of the other, and each exerts its true vapor pressure at the prevailing temperature. When the sum of the separate vapor pressures (of NAPL and water) equals the total pressure, then the mixture boils, and the vapor composition is calculated by the simple gas law. By

Table 2 Physical and chemical properties of NAPL compounds

Property	Methyl cyclohexane	1,2,4-Trimethyl benzene	<i>n</i> -C10	<i>n</i> -C12
Mole fraction in NAPL	0.269	0.220	0.279	0.232
Molecular formula	C ₇ H ₁₄	C ₉ H ₁₂	C ₁₀ H ₂₂	C ₁₂ H ₂₆
Molar mass, g/mol	98.2	120.2	142.3	170.3
Density (T=25°C) kg/m ³	774	880	730	750
Viscosity (T=20°C; (mPa s)	0.735	1.01	0.921	1.49
Normal boiling point (°C)	101	169	174.1	216.2
Vapor pressure at 92°C (mmHg)*	600.7	65.1	52.1	11.5
Solubility in water, mg/L	14.6 (25°C) 20.1 (65°C) 36.2 (95°C)	56.5 (25°C) 62.1 (35°C)	0.015 (25°C)	0.0037 (25°C)

*Calculated by Eq. 3

assuming that NAPL behaves as an ideal liquid and thermodynamic equilibrium, then the partial vapor pressure of each constituent, P_i , is given by Raoult's law, written as

$$P_i = y_i P_m = x_i P_{vi} \tag{1}$$

where y_i , x_i are the mole fractions of compound i in the gas and liquid (NAPL) phases, respectively, P_m is the saturated NAPL vapor pressure, and P_{vi} is the vapor pressure of pure compound i . If the prevailing pressure is P_t , then NAPL will start to boil at the temperature satisfying the condition

$$P_m = P_t - P_w \tag{2}$$

where P_w is the water vapor pressure. Therefore, the boiling point of a mixture of hydrocarbons (NAPL) coexisting with condensed steam is lower than the boiling point of NAPL without steam (steam distillation).

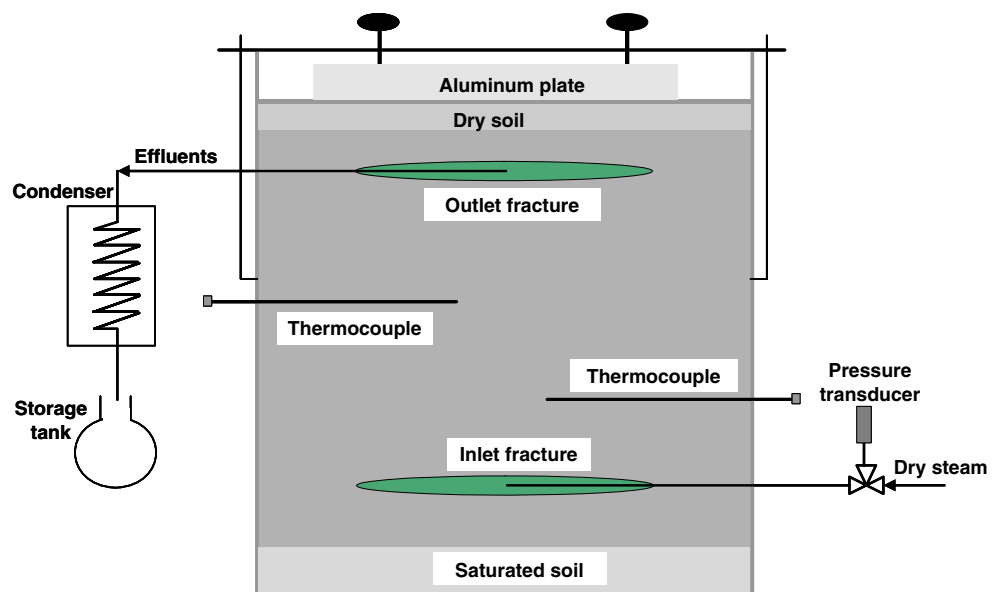
In the steam injection experiment, initially, the gas phase will be enriched with the most volatile compound (methylcyclohexane), and at progressively increasing temperatures (but still less than the normal boiling point of water, 100°C), the less volatile compounds will also vaporize until NAPL stripping is completed. Available experimental data of the vapor pressure vs temperature for the various NAPL compounds over a broad range of temperatures (Perry 1980), were fitted to the following parametric equation (Reid et al. 1977)

$$P_{vi} = \exp \left\{ \frac{1}{T} \left[\frac{A_0}{2} + \sum_{i=1}^n A_i E_i(x) \right] \right\} \tag{3}$$

where the dimensionless temperature x is defined by

$$x = \frac{2T - (T_{\min} + T_{\max})}{T_{\max} - T_{\min}} \tag{4}$$

Fig. 1 Schematic diagram of experimental setup



T_{\min} , T_{\max} are the minimum and maximum temperatures of the dataset, and $E_i(x)$ are Chebyshev polynomials defined by

$$\begin{aligned} E_0(x) &= 1, & E_1(x) &= x, \\ E_{i+1}(x) &= 2xE_i(x) + E_{i-1}(x) \end{aligned} \quad (5)$$

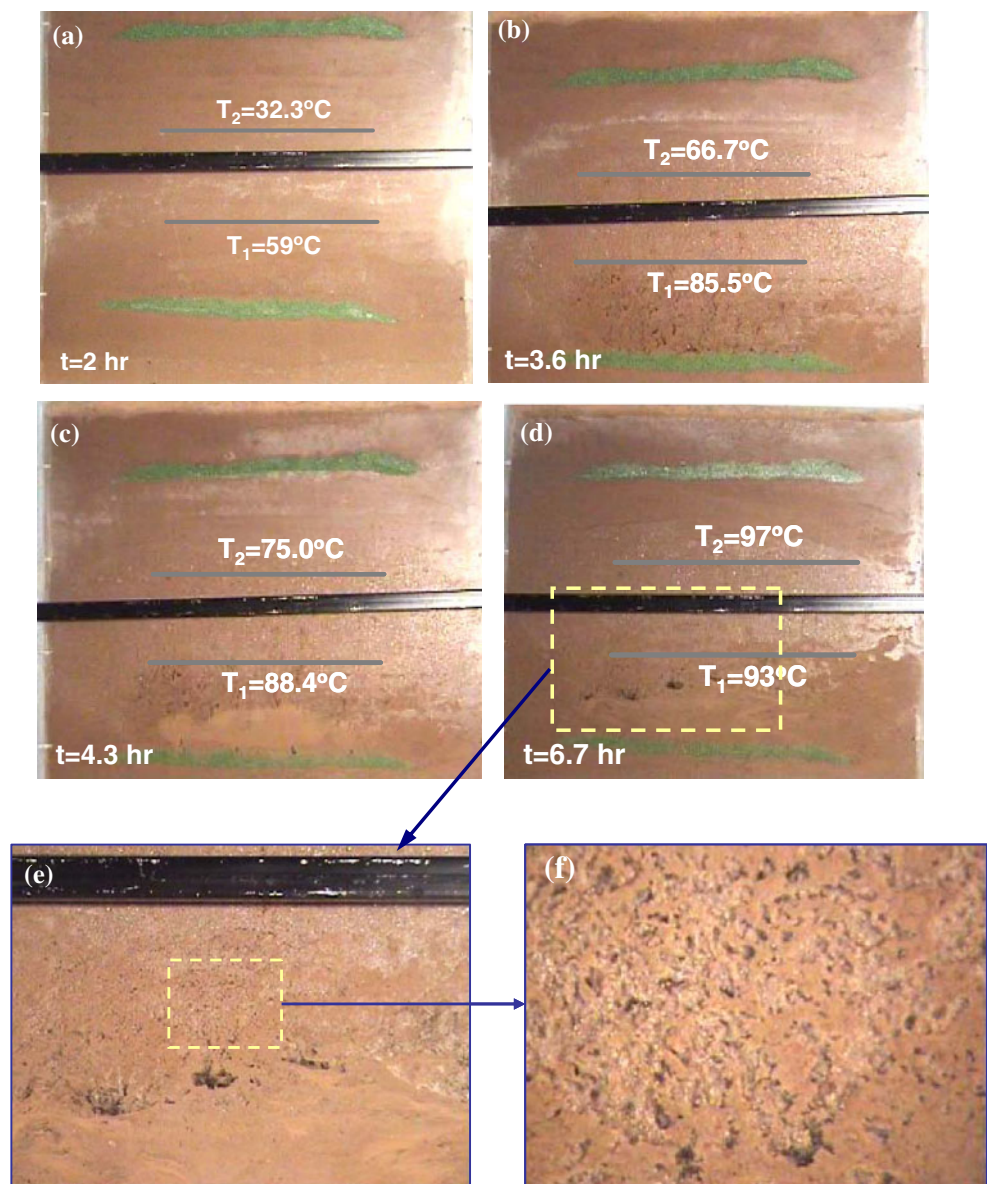
3 Results

3.1 Visualization studies and mechanisms of LNAPL-removal

Snap-shots of the experiment are shown in Fig. 2. Initially, the steam is delivered uniformly across the hydraulic

fracture and is condensed in the colder areas as it flows upwards (see Fig. 2a, b). The soil is unsaturated and gradually the water saturation increases due to steam condensation whereas the temperature of the soil increases (see Fig. 2a–d, Fig. 3a) due to heat conduction and steam convection. Gradually, as water condensation extends to a broad area of the soil, the high water saturation in some areas may reduce substantially the relative permeability of steam and block its convective upward flow (see Fig. 2c). Because of the low permeability of the soil, the steam injection pressure (see Fig. 3b) may be unable to overcome the sum of the critical capillary pressure required for the displacement of water and viscous pressure drop across the condensate. Under such conditions, the rate of the upward convective steam flow becomes nil; the steam is accumulated above the injection

Fig. 2 a–d Successive snap-shots of steam injection test (the front view of soil tank is illustrated); the temperature of the two thermocouples (*gray lines*) is also indicated. e–f Magnified pictures of the soil indicating local details of its pore structure after steam injection



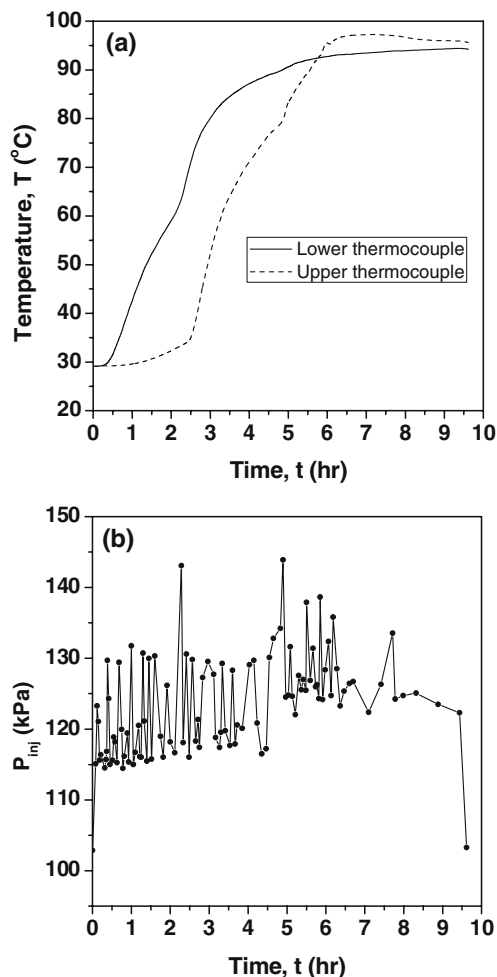


Fig. 3 Transient responses of the **a** soil temperature, measured at two horizontal positions, and **b** steam injection pressure

fracture; the local temperature increases rapidly; water and NAPL start boiling, and locally, the soil is excavated with the opening of micro-fractures (see Fig. 2b–d). With the presence of micro-fractures (see Fig. 2 e, f), the permeability of the soil increases locally (see Fig. 2d), and the flow of steam along with vaporized NAPL is facilitated. Close to the lower thermocouple, the soil has become highly permeable thanks to the creation of micro-fractures (see Fig. 2d). In contrast, at the vicinity of the upper thermocouple, the permeability of the soil is still low (see Fig. 2d). The higher temperature of upper thermocouple may be attributed to the longer retention time of steam in this low-permeability area (see Fig. 2d).

3.2 Estimation of NAPL removal efficiency

The GC-FID analysis of the soil samples revealed a significant decrease in the concentration of all compounds for the majority of soil samples. The removal efficiency of

the various NAPL compounds is an increasing function of their volatility, and exhibits a high spatial variability throughout the soil (Figs. 4 and 5, and Table 3). The remediation is more efficient, and the residual NAPL is smaller in the lower zone surrounding the injection fracture rather than in the upper zone surrounding the extraction fracture (see Figs. 4 and 5). On average, the NAPL removal efficiency is ca. 77% and varies from ca. 73% for the less volatile compound (*n*-C12) to 91% for the most volatile compound [methylcyclohexane (MCE; see Table 3)]. Based on the contours of the removal efficiency (see Figs. 4 and 5), two main areas of relatively low treatment efficiency can be identified: (1) the upper right area of the front side (see Fig. 4a–e); (2) the upper area of the back side (see Fig. 5a–e).

4 Discussion

By using Eqs. 1–5, it was found that the mixture of the four hydrocarbons starts boiling at $T=92^{\circ}\text{C}$ (Fig. 6). This was confirmed experimentally since the earliest drops of condensed mixture of NAPL and water were collected at the outlet after 5.5 h when the soil temperatures $T_1=92^{\circ}\text{C}$ and $T_2=89^{\circ}\text{C}$ were measured with the lower and upper thermocouples (see Fig. 3a), respectively. Afterwards, the amount of condensed NAPL accumulated in the outlet started increasing and steam injection was interrupted after 4 h. The foregoing analysis indicates that steam distillation is the main mechanism of mass-transfer from NAPL to gas phase. Given that vaporization is the dominant mechanism of recovery, the removal efficiency of the various NAPL compounds (see Table 3) follows their volatility (see Table 2).

The rate of NAPL vaporization is enhanced in areas surrounded by preferential flow paths (see Fig. 2b–d) where the high rate of gas flow results in a significant reduction in the concentrations of contaminant vapors (steam stripping) thus increasing the driving force (concentration difference) for mass-transfer from the liquid to the gas phase. The different local vaporization rates, associated with the pore structure heterogeneities, explain the non-uniform spatial distribution of residual NAPL concentration in the soil (see Figs. 4a–e and Fig. 5a–e). In the lower zone, the pore structure of the soil altered substantially, and preferential flow paths were established (see Fig. 2). Instead, no respectable changes of the pore structure were observed in the upper zone (see Fig. 2). The foregoing differences are reflected in the high NAPL-removal efficiency over the lower zone as compared with the low NAPL-removal efficiency over the upper zone (see Fig. 4), particularly with reference to the back side of the soil tank (see Fig. 5).

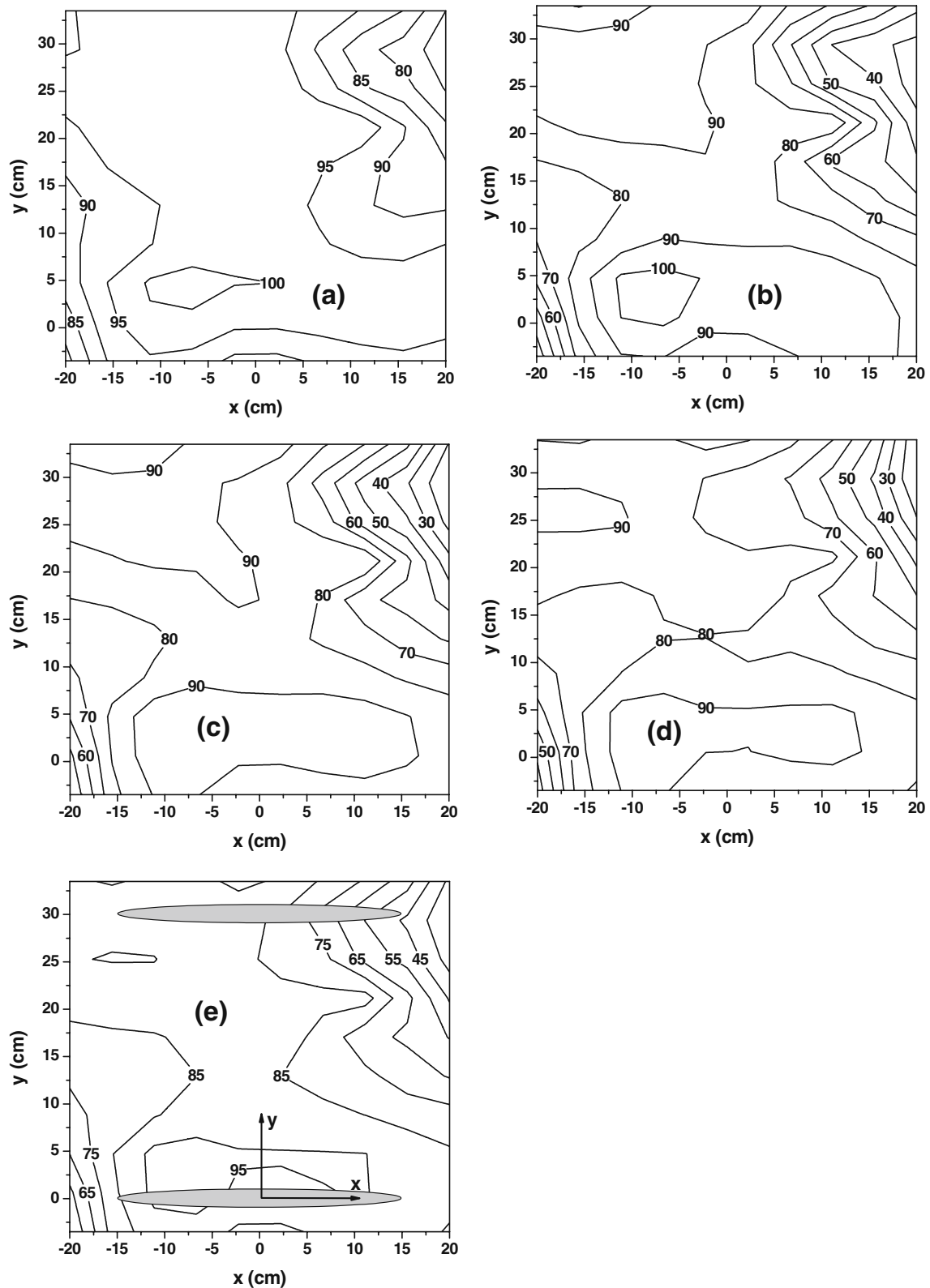


Fig. 4 Equi-percentage contours of NAPL compound removal efficiency for the front side of soil tank. **a** Methylcyclohexane (MCE), **b** 1,2,3-Trimethylbenzene (TMB), **c** *n*-decane (*n*-C10), **d**

n-dodecane (*n*-C12), **e** total NAPL (the position of hydraulic fractures is illustrated)

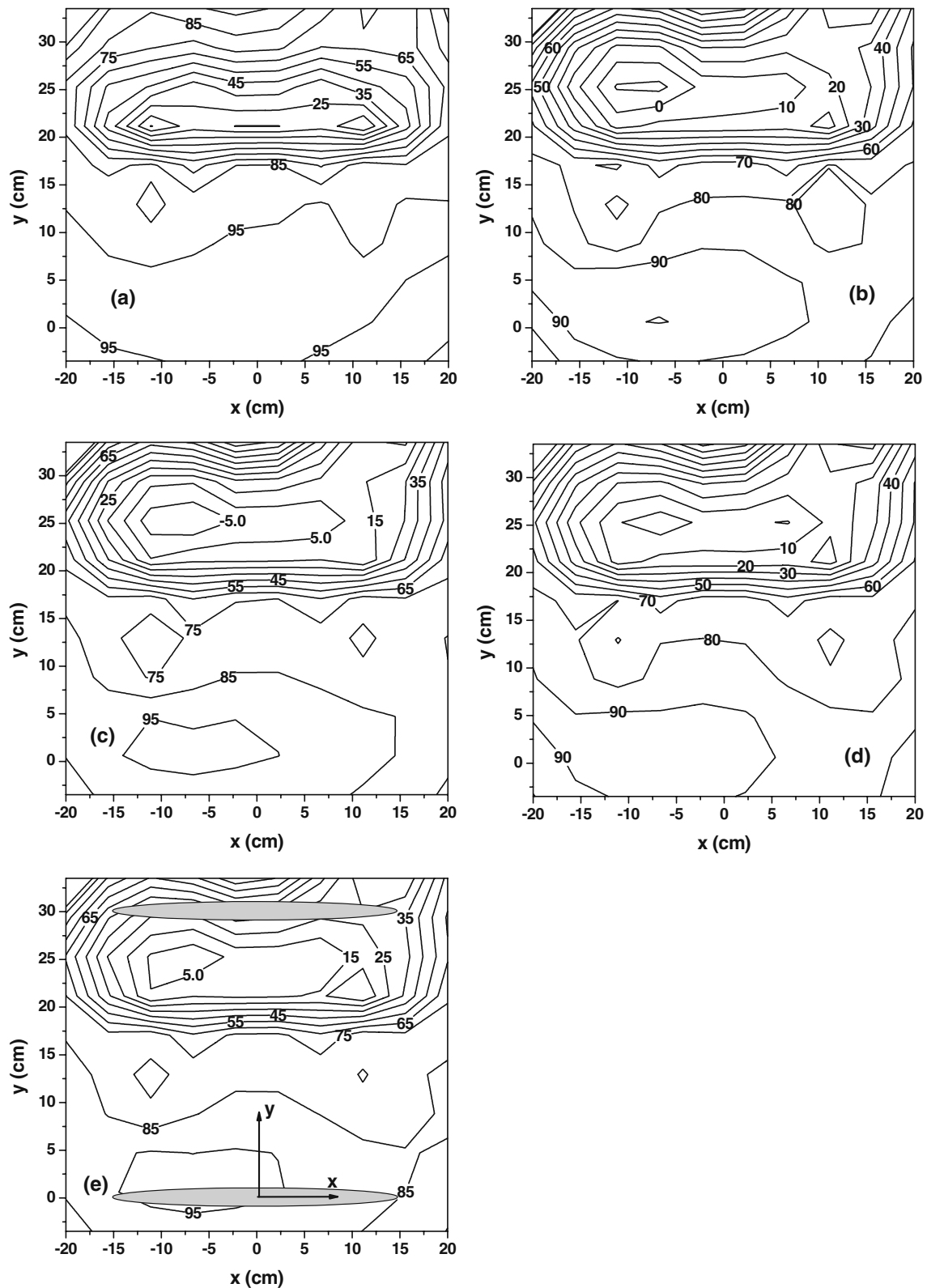


Fig. 5 Equi-percentage contours of NAPL compound removal efficiency from the back side of soil tank. **a** Methylcyclohexane (MCE), **b** 1,2,3-Trimethylbenzene (TMB), **(c)** *n*-decane (*n*-C10), **(d)** *n*-dodecane (*n*-C12), **(e)** total NAPL (the position of hydraulic fractures is illustrated)

Table 3 Statistical moments of the spatial distribution of NAPL compound removal efficiency (%)

NAPL compound	Weight fraction	Front side of soil		Back side of soil		Entire soil	
		Mean value	Standard deviation	Mean value	Standard deviation	Mean value	Standard deviation
MCE	0.2	93.9	6.7	86.8	11.4	90.5	9.8
TMB	0.2	79.8	20.5	69.2	28.1	74.8	24.7
n-C10	0.3	78.8	20.0	68.0	30.2	73.7	25.6
n-C12	0.3	76.8	17.6	68.2	28.2	72.7	23.4
NAPL	1.0	81.4	16.5	72.0	25.3	77.0	21.4

5 Conclusions

A steam injection lab-scale experiment was performed on an unsaturated soil contaminated with a LNAPL composed of four semi-volatile and non-volatile compounds [*n*-C10, *n*-C12, 1,2,4-trimethylbenzene (TMB), and methylcyclohexane (MCE)]. The fluids were injected and extracted through two horizontal coarse-sand lenses acting as hydraulic fractures. The steam flow regime and changes caused on the soil micro-structure were visualized during the experiment. The estimation of NAPL removal efficiency was based on GC-FID chemical analyses of 54 samples collected from various positions of the front and back side of soil after the experiment had been completed.

The NAPL removal efficiency was satisfactory, but non-uniform over the soil, and was maximized for the most volatile compound (methylcyclohexane). Steam injection in the unsaturated zone of a low permeable soil leads to the gradual increase of the local water

saturation, blockage of the upward steam flow, and drastic changes of the pore structure of the soil with the creation of micro-fractures that act as preferential paths for the steam flow. The vaporization of semi-volatile and non-volatile NAPL compounds at temperatures lower than 100°C, thanks to the presence of water (steam distillation), is the main mechanism of NAPL recovery. The stripping of NAPL vapors by flowing steam and subsequent low residual NAPL concentration are favored by the high gas flow rates in areas dominated by preferential flow paths.

6 Recommendations and perspectives

Steam injection combined with hydraulic fracturing can be applied to the unsaturated zone of low-permeability soils for the efficient removal of semi-volatile and non-volatile hydrocarbons (e.g., fuel). Heterogeneities of the void space of soils (e.g., natural fractures) may act as preferential flow paths by minimizing potential changes that might be caused on the pore structure. A pilot-scale remediation experiment was implemented on a highly heterogeneous site polluted heavily by jet fuel (Kluczewo airport situated in North-Western Poland). Except of the different length-scale (laboratory experiment ~0.5 m, field experiment ~10 m), the main difference of the lab-scale tests presented here from the pilot-scale steam injection tests was that, in the second case, the initial distribution of LNAPL (jet fuel) concentration over the site was non-uniform (Tzovolou et al. 2009). Nevertheless, the results of the present study could be employed to interpret the NAPL recovery efficiency of pilot-scale test. There is a need for improving existing numerical models of soil remediation with steam injection by accounting for the steam distillation and potential changes caused on the pore structure and associated with the mechanical properties (e.g., elasticity modulus, stress intensity, etc.) of the soil.

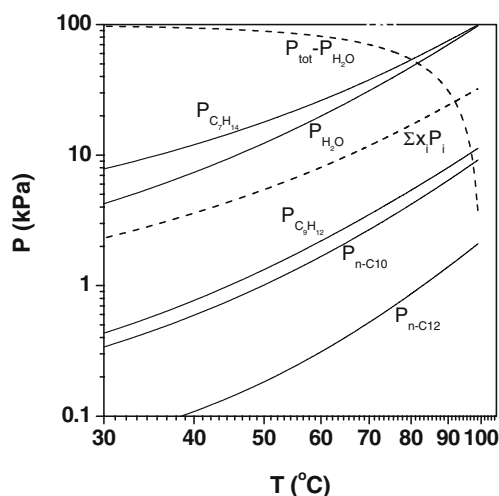


Fig. 6 Vapor pressures of the various compounds (solid lines) and saturated NAPL (dashed lines). The intersection of dashed lines specifies the initial boiling point of NAPL

Acknowledgments This work was performed under Global Change and Ecosystems contract number SSPI-CT-2003-004017-STRESOIL (2004-2007) supported by the European Commission.

References

- Acierno D, Barba AA, d'Amore M, Pinto IM, Fiumara V (2004) Microwaves in soil remediation from VOCs. 2. Buildup of a dedicated device. *AIChE J* 50:722–732
- Aggelopoulos CA, Tsakiroglou CD (2009) A multi-flowpath model for the interpretation of immiscible displacement experiments in heterogeneous soil columns. *J Contam Hydrol* 105:146–160
- Braass O, Tiffert C, Hohne J, Luo X, Niemeyer B (2003) Decontamination of polyaromatic hydrocarbons from soil by steam stripping: mathematical modelling of the mass transfer and energy requirement. *Environ Sci Technol* 37:5001–5007
- Christiansen CM, Riis C, Christensen SB, Broholm MM, Christensen AG, Klint KES, Wood JSA, Bauer-Gottwein P, Bjerg PL (2008) Characterization and quantification of pneumatic fracturing effects at a clay till site. *Environ Sci Technol* 42:570–576
- Class H, Helmig R, Bastian P (2002) Numerical simulation of non-isothermal multiphase multicomponent processes in porous media-I. An efficient solution technique. *Adv Water Resour* 25:533–550
- Davis EL (1998) Steam injection for soil and aquifer remediation. EPA/540/S-97/505
- Dablow JF III, Johnson PC, Pearce JA (2000) In: Balshaw-Biddle K, Oubre CL, Ward CH (eds) Steam and electroheating remediation of tight soils. Lewis Publishers, Boca Raton, Florida, p 410
- Falta RW, Pruess K, Javandel I, Witherspoon PA (1992) Numerical modelling of steam injection for the removal of nonaqueous phase liquids from the subsurface II. Code validation and application. *Water Resour Res* 28:451–465
- Farouq ASM, Meldau RF (1979) Current steamflood technology. *J Pet Technol* 31:1332–1342
- Gudbjerg J, Trotschler O, Farber A, Sonnenborg TO, Jensen KH (2004a) On spurious water flow during numerical simulation of steam injection into water-saturated soil. *J Contam Hydrol* 75:297–318
- Gudbjerg J, Sonnenborg TO, Jensen KH (2004b) Remediation of NAPL below the water table by steam-induced heat conduction. *J Contam Hydrol* 72:207–225
- Hadim A, Shah FH, Korfiatis GP (1993) Laboratory studies of steam stripping of LNAPL-contaminated soils. *J Soil Contam* 2:37–58
- Harrar WG, Murdoch LC, Nilsson B, Klint KES (2007) Field characterization of vertical bromide transport in a fractured glacial till. *Hydrogeol J* 15:1473–1488
- Heron G, Carroll S, Nielsen SGD (2005) Full-scale removal of DNAPL constituents using steam enhanced extraction and electrical resistance heating. *Ground Water Monit R* 25:92–107
- Hunt JR, Sitar N, Udell KS (1988) Nonaqueous phase liquid transport and cleanup, 2. Experimental studies. *Water Resour Res* 24:1259–1269
- Hønning J, Broholm MM, Bjerg P (2007) Role of diffusion in chemical oxidation of PCE in a dual permeability system. *Environ Sci Technol* 41:8426–8432
- Hossain MM, Rahman MK, Rahman SS (2000) Hydraulic fracture initiation and propagation: roles of wellbore trajectory, perforation and stress regimes. *J Pet Sci Eng* 27:129–149
- Kuhlman MI (2002) Analysis of the steam injection at the Visalia Superfund Project with fully compositional nonisothermal finite difference simulations. *J Hazardous Mat* 92:1–19
- Mercer JW, Cohen RM (1990) A review of immiscible fluids in the subsurface: properties, models, characterization and remediation. *J Contam Hydrol* 6:107–163
- Murdoch LC (1995) Forms of hydraulic fractures created during a field test in fine-grained glacial drift. *Q J Eng Geol* 28:23–35
- Perry RH, Chilton CH (1980) *Chemical Engineers' Handbook*, 5th ed., McGraw Hill, New York, pp 3/49–3/68
- Reid RC, Prausnitz JM, Sherwood TK (1977) *The properties of gases and liquids*, 3rd edn. McGraw-Hill, New York, pp 192–193
- Schmidt R, Gudbjerg J, Sonnenborg TO, Jensen KH (2002) Removal of NAPLs from the unsaturated zone using steam: prevention of downward migration by injecting mixtures of steam and air. *J Contam Hydrol* 55:233–260
- She HY, Sleep BE (1998) The effect of temperature on capillary pressure-saturation relationships for air-water and perchloroethylene-water systems. *Water Resour Res* 34:2587–2597
- Slough KJ, Sudicky EA, Forsyth PA (1999) Numerical simulation of multiphase flow and phase partitioning in discretely fractured geologic media. *J Contam Hydrol* 40:107–136
- Stewart LD, Udell KS (1988) Mechanisms of residual oil displacement by steam injection. *SPE Reserv Eng* 3:1233–1242
- Totsche KU, Kogel-Knabner I, Haas B, Gelsen S, Scheibke R (2003) Preferential flow and aging of NAPL in the unsaturated soil zone of a hazardous waste site: implications for contaminant transport. *J Plant Nutr Soil Sci* 166:102–110
- Tse KKC, Lo SL, Wang JWH (2001) Pilot study of in-situ thermal treatment for the remediation of pentachlorophenol-contaminated aquifers. *Environ Sci Technol* 35:4910–4915
- Tzovolou DN, Benoit Y, Haeseler F, Klint KE, Tsakiroglou CD (2009) Spatial distribution of jet fuel in the vadoze zone of a heterogeneous and fractured soil. *Sci Total Environ* 407:3044–3054